DOI: 10.1002/ejic.200700743

Decomposition Cascades of Dicoordinate Copper(I) Chalcogenides

Heiko Jacobsen*[a][‡] and Mark J. Fink[b]

Keywords: Bond energy / Copper / Chalcogens / Density functional calculations / Dispersive interactions

Cu–E, Si–E, and Cu–P bond energies of $R_3PCuESiR_3$ and $CuESiR_3$ complexes (E = O, S, Se) have been investigated using PBE density-functional calculations, and including empirical corrections for dispersive interactions (DFT-D). The bond energies have been used to investigate likely pathways of molecular decomposition. The energy profile for thermal decomposition is to a large degree independent of the nature of the phosphane ligands and silyl groups. Oxides, sulfides, and selenides have qualitatively the same thermal decomposition profile. Thermal decomposition is not likely to produce copper chalcogenide units CuE, but elemental copper Cu instead. Consideration of intermolecular van der Waals attraction suggests that the linear geometry of system tBu$_3$PCuOSiPh$_3$ as found in the crystal is most likely due to crystal packing and intermolecular forces.

1. Introduction

Copper(I) oxide and chalcogenide complexes find extensive usage in a broad variety of applications ranging from catalysis[1] over photovoltaic devices[2,3] to metallaprotein models.[4] In addition, this class of compounds displays a rich chemistry with a great diversity of stoichiometries and geometries, which is governed by the ability of the group 16 element to adopt either terminal or bridging coordination modes. Variations in the ligand framework around the copper center lead to polymeric or oligomeric cluster compounds,[5] structures with a cyclic Cu_2E_2 core,[6] and monomeric complexes.[7]

Copper also plays a major role in meeting the challenges of ever increasing requirements for electrical performance of on-chip wiring, because it is a key element of the interconnection network on a chip of high-performance semiconductor components.[8] One key technique in the design of such devices is chemical vapor deposition (CVD), and with the synthesis of new copper complexes that can be used in CVD applications, coordination chemistry is stretching the limits of micro-electronics technology.[9]

Recently, we reported the synthesis and characterization of the first triad of monomeric dicoordinate copper(I) chalcogenide complexes tBu$_3$PCuESiPh$_3$ (**1**, E = O; **2**, E = S; **3**, E = Se).[10] The X-ray analyses of the copper silylchalcogenolates reveal significant structural structure differences originating from the nature of the chalcogen atom E. The oxygen atom in complex **1** has a linear coordination geometry in contrast to the highly bent sulfur and selenium analogs, **2** and **3**.

In a first theoretical analysis of dicoordinate copper(I) chalcogenides we have performed a detailed analysis of the structure and bonding of representative $H_3PCuESiH_3$ and $CuESiH_3$ model complexes.[11] In the present work, we focus on the thermochemistry of Cu–P, Cu–E, and Si–E bonds in this class of compounds. It is hoped that elucidation of possible decomposition cascades will provide valuable insight into the CVD applicability of copper chalcogenides. In addition, we provide an analysis and rationale of the unexpected molecular geometry of tBu$_3$PCuOSiPh$_3$ **1** as found in the solid state.

2. Results and Discussion

The Cu–P, Cu–E, and Si–E bond energies for a variety of dicoordinate copper(I) chalcogenides have been investigated. The compound numbering of our model complexes is illustrated in Scheme 1.

Bond energies for Cu–P, Cu–E, and E–Si bonds have been estimated from dissociation enthalpies in the gas phase. For calculations of the bond-dissociation enthalpies at 0 K, ΔH^0, reactants and products have been considered to adopt the geometry and electronic structure of their ground states. The decomposition pathways considered in this work are outlined on Scheme 2.

2.1 The Copper–Phosphane Bond: We begin our discussion with a detailed analysis of the Cu–P bond. The bond properties of the phosphane ligand have received considerable attention in the literature, and various concepts

[a] KemKom,
Libellenweg 2, 25917 Leck, Nordfriesland, Germany
E-mail: jacobsen@kemkom.com
[b] Department of Chemistry, Tulane University,
6400 Freret St., New Orleans, LA 70118, USA
[‡] Current address: Department of Chemistry, Tulane University,
6400 Freret St., New Orleans, LA 70118, USA
E-mail: jheiko@tulane.edu

Supporting information for this article is available on the WWW under http://www.eurjic.org or from the author.

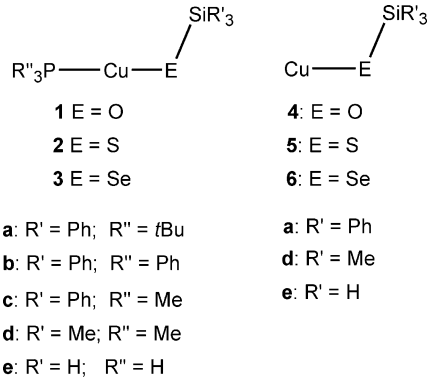

Scheme 1.

like the Tolman angle,[12] basicity parameters[13] or the lone-pair energy of the phosphane donor[14] find extensive use to predict and reason the bonding behavior of phosphanes toward transition-metal fragments. Here, we shall look at bond-dissociation enthalpies ΔH^0, and we will make use of a partitioning of the so called bond-snapping energy BE_{snap}[15] into orbital contributions ΔE_{int} and steric terms ΔE^0. The bond-snapping energy describes the interaction of two suitably prepared fragments, having the right geometry of the final molecule and an electron configuration that allows for bond formation. We model the Cu–P as donor–acceptor bond, and Cu–E and Si–E bonds as covalent bonds formed in the coupling of two radical fragments. In this work, BE_{snap} contains an additional contribution due to dispersive interactions E_{disp} between the phosphane ligands and the silyl groups, and the breakdown that is used here is given in Equation (1).

$$BE_{snap} = -[\Delta E^0 + \Delta E_{int} + E_{disp}] \quad (1)$$

We have drawn on this analysis extensively in our previous work on copper chalcogenide complexes,[11] and in addition we refer the reader to the literature[16] for a detailed account of the energy decomposition scheme employed in this work.

Bond-dissociation enthalpies ΔH^0 and bond-snapping energies BE_{snap} are collected in Table 1. Also included are the individual contributions to BE_{snap} due to steric interaction ΔE^0, orbital interaction ΔE_{int}, and dispersive interaction E_{disp}.

Table 1. Energy terms (in kJ/mol) for the Cu–P bond of various copper(I) chalcogenides.

	ΔE^0	ΔE_{int}	E_{disp}	BE_{snap}	ΔH^0
1a	–59	–203	–8	270	268
1b	–17	–221	–13	251	250
1c	–59	–182	–3	244	245
1d	–48	–178	–1	227	213
1e	–17	–171	0	188	173
2a	–38	–194	–10	242	235
2b	–4	–207	–14	225	220
2c	–40	–172	–4	216	212
2d	–29	–165	–1	195	183
2e	1	–155	0	154	140
3a	–30	–195	–11	236	233
3b	0	–199	–11	210	209
3c	–32	–176	–6	214	212
3d	–23	–165	–1	189	177
3e	5	–153	0	148	136

The bond-dissociation enthalpies follow the expected trend O > S ≈ Se; the ΔH^0 values for the oxygen compounds are about 30 kJ/mol larger than those for the heavier chalcogenides. Within a series of chalcogenide compounds, the bond-dissociation enthalpies span a range of about 130 kJ/mol, where the P*t*Bu$_3$ compounds define the higher end, and the PH$_3$ complexes the lower end of the scale. Overall, the values are in good agreement with bond-dissociation enthalpies at 0 K. Discrepancies arise due to the fact that the geometric preparation energy[15] has not been accounted for, but the overall agreement justifies the derivation of trends based on a more detailed analysis of the bond-snapping energy BE_{snap}.

When we consider the individual components of the bond-snapping energy, we notice that the steric interaction ΔE^0 constitutes a bonding rather than repulsive interaction. This indicates that attractive electrostatic interaction outweighs the contribution of the Pauli repulsion. The magnitude of the stabilizing steric interaction terms of the phosphane ligands PR$_3$″ can be ordered in terms of the R″ group as *t*Bu > Me > Ph > H. This trend correlates well with the accepted basicity of the phosphane ligands.[13] When the silyl group carries methyl rather than phenyl substituents, both the PR$_3$′′ ligand and the SiR$_3$ group compete for electrostatic interaction with the chalcogenide–metal core CuE. As a consequence, ΔE^0 for the PMe$_3$ ligand is reduced

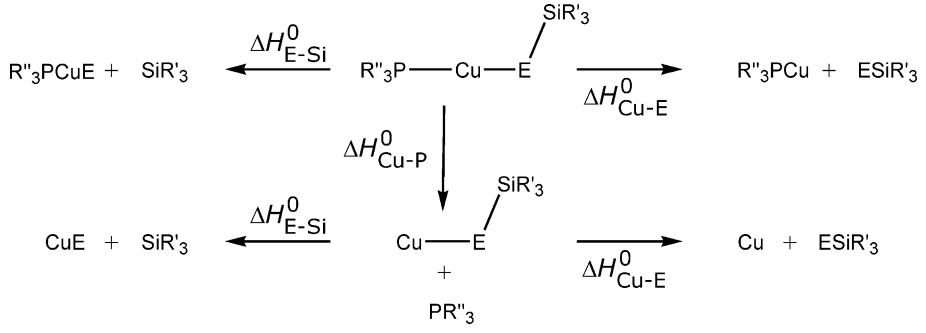

Scheme 2.

(compare entries **1c** and **1d**, **2c** and **2d**, **3c** and **3d** in Table 1).

The major contribution to BE_{snap} arises from the orbital interaction energy ΔE_{int}. If we extend the basicity arguments and restrict the interaction between a phosphane ligand and a copper–chalcogenide core to electron donation only, the phosphane lone-pair energies provide a measure of the ligand donor strength, and thus a measure of ΔE_{int}. We then would expect the same qualitative ranking found for the steric interaction to be reciprocated in the orbital interaction: *t*Bu > Me > Ph > H. Inspection of the data in Table 1, however, indicates that the triphenylphosphane ligand unexpectedly shows the strongest orbital interaction.

By now, it is well recognized that the bond between the phosphane ligands and transition-metal fragments contains a sizeable contribution due to π-backdonation,[17] and an early DFT investigation of $(CO)_5Cr(PH_3)$ reports a metal–phosphane bond strength of 144 kJ/mol, with a contribution of about 25% attributed to π-backdonation.[18] Employing orbital-based arguments, the amount of backdonation between [P] and [CuE] fragments is qualitatively represented by the $HOMO_{[CuE]}$–$LUMO_{[P]}$ gap. An orbital analysis of model system has revealed the fact that Cu–E π_{dp}-antibonding orbitals are among the set of highest occupied molecular orbitals of the copper-chalcogenide core, and that backdonation from Cu-based d orbitals to σ* orbitals of the phosphane ligand strengthens the Cu–P bond.[11]

An inspection of the frontier-orbital energies of the phosphane ligands and copper–chalcogenide cores corroborates the trends in Cu–P bonding indicated thus far, and also provides an explanation for the unusually high ΔE_{int} contribution of the PPh_3 ligand. HOMO and LUMO energies for the CuE cores **4a**, **5a**, and **6a** and for the phosphanes PR_3'', R'' = *t*Bu, Ph, Me, H, are depicted in Figure 1.

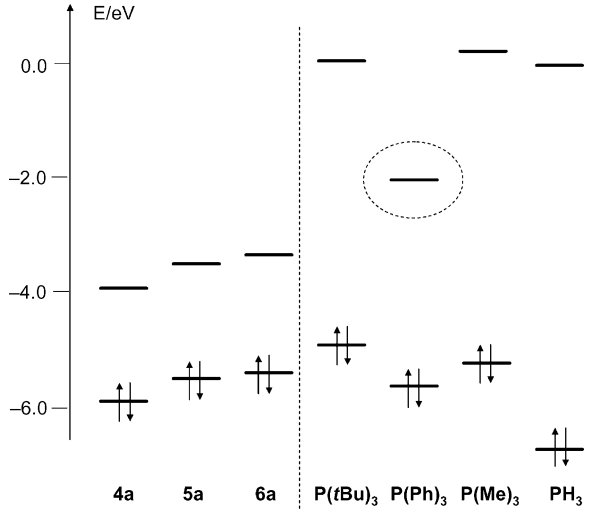

Figure 1. Frontier-orbital energies for copper–chalcogenide fragments (left) and phosphane ligands (right). The LUMO of PPh_3 is at an unexpectedly low energy level (dotted circle).

Trends in basicities correlate well with relative $HOMO_{[P]}$ energies. The LUMO of triphenylphosphane is at exceptionally low energy, which causes a reduced $HOMO_{[CuE]}$–$LUMO_{[P]}$ gap, and consequently enhances the backdonation. This observation accounts for the unexpectedly strong orbital interaction of triphenylphosphane.

When assessing the Cu–P bond strength, it is instructive to compare the Cu–P bond strength for the Cu atom to that for CuE cores. The Cu–P bond strength in H_3P–Cu is calculated to amount to 104 kJ/mol.[19] In contrast, the Cu–P bond-snapping energies BE_{snap} in **1a**, **2a**, and **3a** are stronger by 69, 36, and 32 kJ/mol, respectively. The presence of the chalcogen atom significantly strengthens the Cu–P bond. This is due to backdonation out of filled Cu–E π_{dp}-antibonding orbital into empty σ* orbitals of the phosphane ligand.

Dispersive interactions E_{disp} provide additional bond stabilization of up to 14 kJ/mol for systems with sterically demanding phosphane ligands and large silyl groups. We will return to the importance of dispersive interactions at a later point in our discussion.

2.2 Bonds Involving Chalcogen Atoms: The bond-dissociation enthalpies ΔH^0 of Cu–E and E–Si bonds are displayed in Figure 2. The Cu–E, and E–Si bond strengths follow the expected trend O > S > Se. The silicon–oxygen bond is a strong bond with a dissociation energy of 536 kJ/mol,[20]

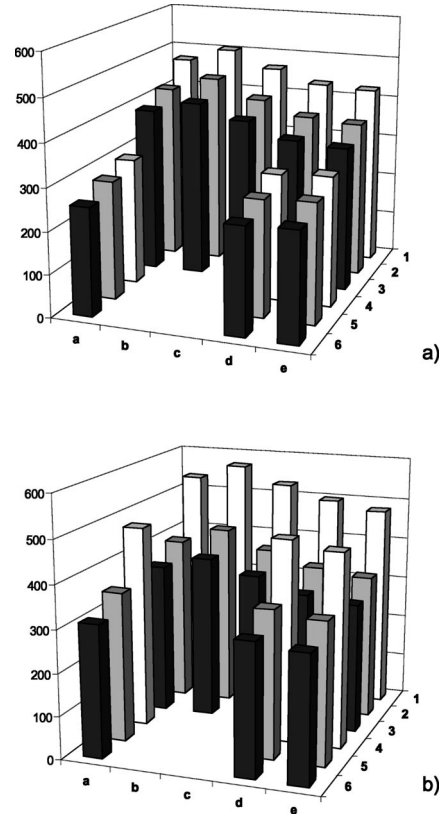

Figure 2. Bond-dissociation enthalpies ΔH^0 (in kJ/mol) of copper–chalcogen bonds (Cu–E; Figure 2, a) and silicon–chalcogen bonds (Si–E; Figure 2, b).

and the O–Si bond-dissociation enthalpies for the copper chalcogenides fall all around this value. When we compare Cu–E bond energies of systems with phosphane ligands (**1**, **2**, **3**) with bond energies of systems without phosphane ligands (**4**, **5**, **6**), we find that coordination of a PR_3 significantly enhances the Cu–E bond strength. For example, if we consider the "real" systems **1a**, **2a**, **3a**, the copper–chalcogenide Cu–E bonds are stronger by 174 kJ/mol (E = O), 141 kJ/mol (E = S) and 138 kJ/mol (E = Se), in comparison to the "phosphane-free" systems **4a**, **5a**, and **6a**.

Not only does the presence of a chalcogen atom strengthen the Cu–P bond, as discussed above, but the presence of a phosphane ligand also induces a stabilization of the Cu–E bond. This synergistic effect is caused by enhanced π-backbonding from the copper center to the phosphane ligand. As mentioned before, Cu–E π_{dp}-antibonding orbitals are among the set of highest occupied molecular orbitals of the Cu–E core. Backdonation from Cu-based d orbitals to σ* orbitals of the phosphane ligand not only strengthens the Cu–P bond, but at the same reduces the antibonding Cu–E interaction and thus strengthens the Cu–E bond.

The Si–E bonding interaction too is enhanced due to the presence of an additional phosphane ligand. This secondary intrinsic effect amounts to 22 kJ/mol (E = O), 10 kJ/mol (E = S) and 9 kJ/mol (E = Se) for model compounds with PH_3 ligands and SiH_3 groups. For real systems with P*t*Bu_3 ligands and $SiPh_3$ groups, this effect is more pronounced and yields a secondary intrinsic stabilization energies of 59 kJ/mol (E = O), 43 kJ/mol (E = S) and 41 kJ/mol (E = Se), respectively.

If we compare relative Si–E and Cu–E bond strengths, we find that for systems without PR_3 ligands, the Si–E bonds are always stronger than the Cu–E bonds. The average energy differences are about 165 kJ/mol for oxygen complexes, but only about 65 kJ/mol and 50 kJ/mol for sulfur and selenium compounds, respectively. When we turn to phosphane complexes, we find modifications in this general trend due to the fact that the presence of phosphorus ligand significantly enhances the Cu–E bond strength. For the O complexes the energy difference between Si–O and Cu–O bonds decreases to about 60 kJ/mol, still in favor of the silicon–oxygen bond. For the heavier chalcogen atoms, the relative bond strengths between Si–E and Cu–E bonds is now inverted; and the S and Se complexes all have Cu–E bonds that are stronger than Si–E bonds by about 25 and 35 kJ/mol, respectively.

When we investigate the influence of the R′ and R′′ ligands on the strength of the Cu–E and Si–E bonds, we find that for phosphane systems these bond energies vary within a range of about 80 kJ/mol. For complexes without an additional phosphane ligand, we find that independent of the nature of the R′ group, for a given chalcogen element the values for Cu–E and Si–E bond-dissociation enthalpies are approximately the same.

2.3 Decomposition Cascades: We are now at a point that we can discuss possible decomposition pathways of dicoordinate copper(I) chalcogenides, Scheme 3.

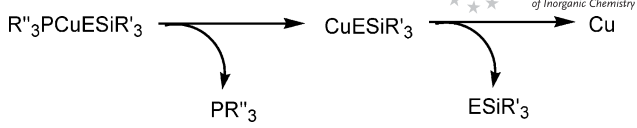

Scheme 3.

For all complexes investigated in the present work, the Cu–P bond always constitutes the weakest link. Thus, thermal decomposition of a dicoordinate copper(I) chalcogenide (DCC) is most likely initiated by dissociation of the phosphane ligand; a process that results in formation of a monocoordinate copper(I) chalcogenide (MCC). For this type of compounds, contrary to DCCs, the Cu–E bond is always weaker than the Si–E bond. Therefore, the second step in thermal decomposition most likely involves cleavage of the Cu–E bond. Thermal decomposition is not likely to produce copper chalcogenide units CuE, but elemental copper Cu instead. Furthermore, the energy profile for thermal decomposition is to a large degree independent of the nature of the phosphane ligands and silyl groups. Oxides, sulfides, and selenides all have qualitatively the same thermal decomposition profile. In addition, sulfides and selenides display approximately the same quantitative thermodynamics.

2.4 The Structure of *t*Bu_3PCuOSiPh_3 in the Gas Phase and in the Solid State: X-ray crystallography has shown that the Cu atoms in the copper silylchalcogenolates *t*Bu_3PCuE-$SiPh_3$ (**1**, E = O; **2**, E = S; **3**, E = Se) have either a linear or a near-linear coordination geometry in all three complexes. Interestingly, the O atom in complex **1** is also linear, which is in contrast to the highly bent S and Se analogs, compounds **2** and **3**, respectively.[10] Our initial calculations on H_3PCuESiH_3 model compounds have indicated that the unusual geometry of the oxygen compound **1** is not caused by intermolecular orbital interactions such as extended π-delocalization, but are the result of a fine balance of electrostatic interaction and Pauli repulsion.[11] In the last section of this work, we will address the unusual solid-state structure of *t*Bu_3PCuE$SiPh_3$ (**1a**) in more detail.

Our geometry optimization of **1a**, the gas-phase analog of the solid-state structure **1**, resulted in a bent geometry with an angle ∠(Cu–O–Si) of 117°. In addition, we optimized a linear structure **1a**′ by fixing the angle ∠(Cu–O–Si) at 180°. In the gas phase, the linear structure is 23 kJ/mol higher in energy compared to the bent ground state geometry, and an energy partitioning for the linearization process is outlined in Figure 3.

When complex **1a** takes on a linear, rather than a bent geometry, the distance between the P and Si centers of the sterically demanding peripheral ligands increases from 493 pm to 556 pm, and Pauli repulsion is reduced. As a consequence, the linear geometry is favored in terms of the steric interaction ΔE^0. However, the orbital interactions ΔE_{int} as well as dispersive interaction are stronger in a bent arrangement, and as a consequence, the linear structure **1a**′ is higher in energy.

Our calculations indicate that the dispersive interactions E_{disp} lead to an increase in bond energy in **1a** and therefore

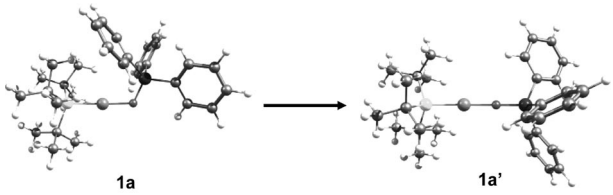

ΔE^0 = –40 kJ/mol; ΔE_{int} = 56 kJ/mol; ΔE_{disp} = 7 kJ/mol; ΔE = 23 kJ/mol

Figure 3. Bond linearization of tBu$_3$PCuOSiPh$_3$ in the gas phase.

to a larger barrier to planarity. We attribute this increase to an enhanced long-range $1/r^6$-induced dipole-induced dipole attraction. van der Waals forces not only incorporate short-range exponential repulsion arising from Pauli orthogonalization, but long-range dispersive attraction as well. Due to the large separation of the sterically demanding ligands, the long-range attraction outweighs the short-range repulsion, and nonbonded interactions strengthen, but not weaken, the Cu–P, Cu–E, and Si–E bonds.

Although the barrier to planarity is increased due to *intramolecular* dispersive attraction, in the crystal there exists the possibility of *intermolecular*, long-range dispersive interaction, which might lower the barrier to planarity or even favor a linear coordination geometry over a bent arrangement.

Compound **1** crystallizes in the highly symmetric space group $P\bar{3}$, in which the linear P–Cu–O–Si skeleton lies exactly on a crystallographic threefold rotation axis. The crystal packing for **1** is displayed in Figure 4; also indicated are neighboring phosphane ligands and silyl groups that give rise to dispersive stabilization.

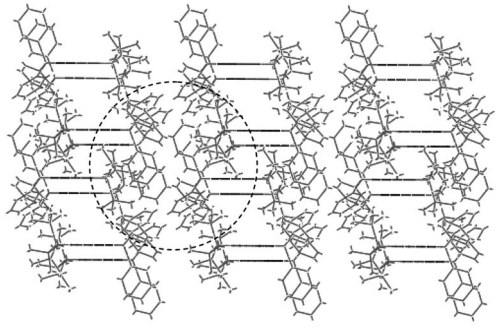

1a(bent, solid state) → **1a'**(linear, solid state) ΔE_{disp} = –28 kJ/mol

Figure 4. Crystal packing of tBu$_3$PCuOSiPh$_3$. Neighboring phosphane ligands and silyl groups from different molecular units undergo dispersive interaction (dotted circle).

We have calculated intermolecular dispersion energies for the linear geometry **1a**′ based on the crystal structure of **1**. The dispersion forces in the solid state for a bent geometry **1a** were modeled after the crystal structure of the sulfur analog, and if we compare the dispersive lattice energies we find that the linear arrangement is favored over a packing of a bent molecular unit by 28 kJ/mol per molecule. The energetic stabilization of a linear arrangement due to packing forces slightly outweighs the preparation energy required to distort the bent structure and we conclude that the unusual molecular structure of tBu$_3$PCuOSiPh$_3$ as observed in the solid state results from crystal packing, and is not an indication of unusual intermolecular bonding.

Molecular structures as obtained from crystal structure analysis are not always good representations for the geometry of the isolated and unperturbed molecule. If the potential energy surface of internal molecular coordinates is shallow and does not display a pronounced minimum, intermolecular dispersive forces as well as intermolecular electrostatic interaction[21] might significantly influence the geometry of the molecular unit in the solid state.

3. Conclusion

As stated in the introduction, one of the main goals of the present work was to elucidate the CVD applicability of copper chalcogenides, and in conclusion of this work, we shall summarize our findings with respect to this question. We found that the energy profile for thermal decomposition is to a large degree independent of the nature of the phosphane ligands and silyl groups. We also found that oxides, sulfides, and selenides have qualitatively the same thermal decomposition profile.

A minor aspect of the current work was the analysis and rationalization of the unexpected molecular geometry of tBu$_3$PCuESiPh$_3$ as found in the solid state. Consideration of intermolecular van der Waals attraction suggests that the linear geometry of system tBu$_3$PCuOSiPh$_3$ as found in the crystal is most likely due to crystal packing and intermolecular forces.

4. Computational Details

Density-functional calculations have been carried out using the Amsterdam Density Functional ADF suite of programs, version ADF2006.01.[22] The calculation were based on the local-density approximation with Slater exchange[23] and VWN-V correlation.[24] Gradient corrections as proposed by Perdew, Burke and Enzerhof[25] have been added self-consistently.

Molecular orbitals were expanded in an uncontracted set of Slater-type orbitals (STOs). For H and C the basis used was of double-ζ quality, whereas for O, Si, P, S, and Se a triple-ζ basis has been employed, and both basis sets were augmented with one set of polarization functions (ADF basis sets III and IV, respectively). The transition metal was described by a triple-ζ basis augmented with two sets of polarization functions (ADF basis set V). The core shells (C, O: 1s; Si, P, S, Cu: 1s2s2p; Se: 1s2s2p3s3p3d) were treated by the frozen-core approximation, and an auxiliary set of s, p, d, f and g STOs was used to fit the molecular density and to represent the Coulomb and exchange potentials accurately in each SCF cycle.[26]

Geometries have been optimized according to the method developed by Versluis and Ziegler.[27] Frequencies for molecules with R′ = R′′ = H have been calculated analytically,[28] and served as basis for zero-point-energy corrections. Empirical corrections for intramolecular dispersive forces between SiR_3' groups and PR_3'' ligands have been included for geometry optimization and energy calculations (DFT-D).[29]

Intermolecular dispersive interactions in the crystal have been calculated with the Generalized Lattice Utility Program GULP.[30] These calculations employ an undamped dispersion potential of the form suggested by Tang and Toennies.[31]

The consistency of the density functional calculations has been checked by single point calculations using other pure and hybrid density functionals, as well as different basis sets. These calculations are documented in the Supporting Information.

Supporting Information (see also the footnote on the first page of this article): Cartesian coordinates and final energies for optimized complexes. Results of consistency calculations.

Acknowledgments

We gratefully acknowledge Prof. L. Cavallo for granting access to the MoLNaC Computing Facilities at Dipartimento di Chimica, Università di Salerno.

[1] R. Grigg, D. M. Cooper, S. Holloway, S. McDonald, E. Millington, M. A. B. Sarker, *Tetrahedron* **2005**, *81*, 8677–8685; V. Percec, C. Grigoras, *J. Poly. Sci., Part A* **2005**, *43*, 3920–3931; A. Corma, A. E. Palomares, F. Rey, F. Márquez, *J. Catal.* **1997**, *170*, 140–149; J. Linder, M. A. V. Garcia, A. Achdev, J. Schwank, *J. Chem. Soc. Chem. Commun.* **1989**, 1833–1835.
[2] T. Komuro, H. Kawaguchi, K. Tatsumi, *Inorg. Chem.* **2002**, *41*, 5083–5090.
[3] W. Hirpo, S. Dhingra, A. C. Sutorik, M. G. Kanatzidis, *J. Am. Chem. Soc.* **1993**, *115*, 1597–1599; K. K. Banger, J. A. Hollingsworth, J. D. Harris, J. Cowan, W. E. Buhro, A. F. Hepp, *Appl. Organomet. Chem.* **2002**, *16*, 617–627; R. P. Raffaelle, S. L. Castro, A. F. Hepp, S. G. Bailey, *Prog. Photovolt. Res. Appl.* **2002**, *10*, 433–439; B. J. Stanbery, *Crit. Rev. Solid State Mater. Sci.* **2002**, *27*, 73–117.
[4] D. R. Winge, C. T. Dameron, G. N. George, I. J. Pickering, I. G. Dance, *Bioinorg. Chem. Copper* **1993**, 110–123.
[5] I. G. Dance, M. L. Scudder, L. J. Fitzpatrick, *Inorg. Chem.* **1985**, *24*, 2547–2550.
[6] X.-Y. Liu, F. Mota, P. Alemany, J. J. Novoa, S. Alvarez, *Chem. Commun.* **1998**, 1149–1150.
[7] D. T. T. Tran, N. J. Taylor, J. F. Corrigan, *Angew. Chem. Int. Ed.* **2000**, *39*, 935–937; D. T. T. Tran, J. F. Corrigan, *Organometallics* **2000**, *19*, 5202–5208.
[8] K. Maex, M. R. Baklanov, D. Shamiryan, F. Iacopi, S. H. Brongersma, Z. S. Yanovitskaya, *J. Appl. Phys.* **2003**, *93*, 8793–8841.
[9] P. Doppelt, *Coord. Chem. Rev.* **1998**, *178*, 1785–1809; Y. B. Dong, M. D. Smith, R. C. Layland, H. C. zur Loye, *Inorg. Chem.* **1999**, *38*, 5027–5033.
[10] I. Medina, H. Jacobsen, J. T. Mague, M. J. Fink, *Inorg. Chem.* **2006**, *45*, 8844–8846.
[11] H. Jacobsen, M. J. Fink, *Inorg. Chim. Acta* **2007**, *360*, 3511–3517.
[12] C. A. Tolman, *Chem. Rev.* **1977**, *77*, 313–348.
[13] S. Joerg, R. S. Drago, J. Sales, *Organometallics* **1998**, *17*, 589–599.
[14] H. M. Senn, D. V. Deubel, P. E. Blöchl, A. Togni, G. Frenking, *J. Mol. Struct. THEOCHEM* **2000**, *506*, 233–242.
[15] H. Jacobsen, T. Ziegler, *Comments Inorg. Chem.* **1995**, *17*, 301–307.
[16] F. M. Bickelhaupt, E. J. Baerends, *Rev. Comput. Chem.* **2000**, *15*, 1–86.
[17] G. Frenking, K. Wichmann, N. Fröhlich, C. Loschen, M. Lein, J. Frunzke, V. M. Rayón, *Coord. Chem. Rev.* **2003**, *238*, 55–82.
[18] H.-B. Kraatz, H. Jacobsen, T. Ziegler, P. M. Boorman, *Organometallics* **1993**, *12*, 76–80.
[19] G. A. Bowmaker, M. Pabst, N. Rösch, H. Schmidbauer, *Inorg. Chem.* **1993**, *32*, 880–887.
[20] K. M. Downard, J. H. Bowie, R. N. Hayes, *Aust. J. Chem.* **1990**, *43*, 511–520.
[21] H. Jacobsen, T. Brackemeyer, H. Berke, G. Erker, R. Fröhlich, *Eur. J. Inorg. Chem.* **2000**, 1423–1428
[22] G. te Velde, F. M. Bickelhaupt, S. J. A. van Gisbergen, C. Fonseca Guerra, E. J. Baerends, J. G. Snijders, T. Ziegler, *J. Comput. Chem.* **2001**, *22*, 931–967; C. Fonseca Guerra, J. G. Snijders, G. te Velde, E. J. Baerends, *Theor. Chem. Acc.* **1998**, *99*, 391–403. ADF2006.01, SCM, Theoretical Chemistry, Vrije Universiteit, Amsterdam, The Netherlands.
[23] J. C. Slater, *Phys. Rev.* **1951**, *81*, 385–390.
[24] S. H. Vosko, L. Wilk, M. Nusair, *Can. J. Phys.* **1980**, *58*, 1200–1211.
[25] J. P. Perdew, K. Burke, M. Ernzerhof, *Phys. Rev. Lett.* **1996**, *77*, 3865–3868; J. P. Perdew, K. Burke, M. Ernzerhof, *Phys. Rev. Lett.* **1997**, *78*, 1396.
[26] E. J. Baerends, D. E. Ellis, P. Ros, *Chem. Phys.* **1973**, *2*, 41–51.
[27] L. Versluis, T. Ziegler, *J. Chem. Phys.* **1988**, *88*, 322–328.
[28] S. K. Wolff, *Int. J. Quantum Chem.* **2005**, *104*, 645–659; H. Jacobsen, A. Berces, D. P. Swerhone, T. Ziegler, *Comput. Phys. Commun.* **1997**, *100*, 263–276; A. Berces, R. M. Dickson, L. Y. Fan, H. Jacobsen, D. P. Swerhone, T. Ziegler, *Comput. Phys. Commun.* **1997**, *100*, 247–262; H. Jacobsen, A. Berces, D. P. Swerhone, T. Ziegler, *ACS Symp. Ser.* **1996**, *629*, 154–163.
[29] S. Grimme, *J. Comput. Chem.* **2004**, *25*, 1463–1473. J. M. Ducere, L. Cavallo, manuscript in preparation.
[30] J. D. Gale, *J. Chem. Soc. Faraday Trans.* **1997**, *93*, 629–637; J. D. Gale, A. L. Rohl, *Mol. Simul.* **2003**, *29*, 291–341; J. D. Gale, *Z. Kristallogr.* **2005**, *220*, 552–554.
[31] K. T. Tang, J. P. Toennies, *J. Chem. Phys.* **1984**, *80*, 3726–3741.

Received: July 13, 2007
Published Online: October 1, 2007

